Heterologous expression of the *Halothiobacillus neapolitanus* carboxysomal gene cluster in *Corynebacterium glutamicum*

Meike Baumgart[a*], Isabel Huber[a], Iman Abdollahzadeh[b,c], Thomas Gensch[b], Julia Frunzke[a*]

[a] Institute of Bio- and Geosciences, IBG-1: Biotechnology, Forschungszentrum Jülich, Jülich, Germany

[b] Institute of Complex Systems (ICS-4 (Cellular Biophysics)), Forschungszentrum Jülich, Jülich, Germany

[c] Institute of Complex Systems (ICS-6 (Structural Biochemistry)), Forschungszentrum Jülich, Jülich, Germany

*Address correspondence to m.baumgart@fz-juelich.de and j.frunzke@fz-juelich.de

Abstract

Compartmentalization represents a ubiquitous principle used by living organisms to optimize metabolic flux and to avoid detrimental interactions within the cytoplasm. Proteinaceous bacterial microcompartments (BMCs) have therefore created strong interest for the encapsulation of heterologous pathways in microbial model organisms. However, attempts were so far mostly restricted to *Escherichia coli*. Here, we introduced the carboxysomal gene cluster of *Halothiobacillus neapolitanus* into the biotechnological platform species *Corynebacterium glutamicum*. Transmission electron microscopy, fluorescence microscopy and single molecule localization microscopy suggested the formation of BMC-like structures in cells expressing the complete carboxysome operon or only the shell proteins. Purified carboxysomes consisted of the expected protein components as verified by mass spectrometry. Enzymatic assays revealed the functional production of RuBisCO in *C. glutamicum* both in the presence and absence of carboxysomal shell proteins. Furthermore, we could show that eYFP is targeted to the carboxysomes by fusion to the large RuBisCO subunit. Overall, this study represents the first transfer of an α-carboxysomal gene cluster into a Gram-positive model species supporting the modularity and orthogonality of these microcompartments, but also identified important challenges which need to be addressed on the way towards biotechnological application.

Keywords: Bacterial Microcompartments, carbon fixation, RuBisCO, *Corynebacterium glutamicum*, Synthetic Biology, BMC

1. Introduction

Spatial organization is used by all living organisms for the optimization of cellular transport and metabolism. The overall concept of encapsulation of metabolic (sub-) pathways has been found in a variety of bacterial species and is realized, for example, by the formation of bacterial microcompartments (BMCs) (Bobik et al., 2015; Kerfeld and Erbilgin, 2015). The spatial separation of distinct cellular processes confers a selective advantage to the particular host, e.g. by avoiding metabolic interference with other cytoplasmic reactions, encapsulation of toxic intermediates, and increasing pathway efficiency by scaffolding of participating enzymes or increasing local substrate concentration.

A typical BMC consists of metabolic enzymes that are encapsulated by proteins forming a shell with selective permeability, which is controlled by specific protein pores within the shell structure. Different studies revealed the presence of more than seven different BMC types in 23 bacterial phyla (Axen et al., 2014; Kerfeld and Erbilgin, 2015). The genomic organization of BMC gene clusters suggests that these genetic modules are frequent targets of horizontal gene transfer (Gupta, 2012). The most extensively studied classes of BMCs are the carboxysomes (Kerfeld and Melnicki, 2016; Rae et al., 2013) as well as the metabolosomes involved in the catabolism of 1,2-propandiol (Pdu), and ethanolamine (Eut) (Bobik et al., 2015; Chowdhury et al., 2014; Frank et al., 2013; Kerfeld and Erbilgin, 2015).

CO_2-fixing carboxysomes are found in almost all cyanobacteria, where they enhance autotrophic growth *via* the Calvin cycle (Rae et al., 2013). In general, both types of carboxysomes (α and β), which show significant differences in components and assembly, consist of a protein shell of polyhedral shape encapsulating the RuBisCO (ribulose-1,5-bisphosphate carboxylase/oxygenase) enzyme and the carbonic anhydrase (Kerfeld and Melnicki, 2016; Rae et al., 2013). Whereas one RuBisCO substrate, ribulose bisphosphate, is freely crossing the carboxysomal shell, CO_2 is produced from bicarbonate in the BMC lumen

by carbonic anhydrase (Badger and Price, 2003). Thus, the protein shell of the carboxysome plays an important role in enhancing RuBisCO activity by increasing the local CO_2 concentration and by acting as a diffusion barrier for O_2, the substrate of photorespiration.

BMCs are nowadays highly interesting for synthetic biology and bioengineering approaches. Detailed insights into the molecular factors contributing to the functional assembly and organization are the key for an understanding of BMC function and transfer into a heterologous background. The formation of α– and β-carboxysomes follows different modes: whereas α-carboxysomes assemble concomitantly with the aggregation of RuBisCO (Iancu et al., 2010), the assembly of β-carboxysomes is initiated by the aggregation of RuBisCO and the CcmM-CcmN complex at the cell poles (Cameron et al., 2013; Kinney et al., 2012). Within the BMC core, RuBisCO is present in a paracrystalline state, which likely contributes to an optimal substrate channeling (Kaneko et al., 2006). The formation of empty compartment shells has been reported for carboxysomes in a *H. neapolitanus* strain lacking the RuBisCO enzyme (Baker et al., 1998; Menon et al., 2008).

Recent studies explored the use of modular BMCs as synthetic nano-bioreactors enhancing small molecule production of microbial strains. As an important groundwork, the α-carboxysome of *H. neapolitanus* was expressed in *Escherichia coli*: correct assembly of the carboxysome and the presence of RuBisCO activity was demonstrated (Bonacci et al., 2012). Further studies reported on the heterologous production of Pdu and Eut metabolosomes in *E. coli* (Choudhary et al., 2012; Parsons et al., 2008). These studies emphasized BMCs, in general, as orthogonal modules for synthetic biology approaches. However, in all cases, BMC gene clusters where transferred from a γ-proteobacterial donor strain to *E. coli*, which is likewise a member of the Gammaproteobacteria. Only the study of Lin *et al.* provided a first proof-of-concept of the expression and assembly of β-carboxysomes in chloroplasts of the plant *Nicotiana benthamiana* (Lin et al., 2014).

In this study, we transferred the α-carboxysomal gene cluster of *H. neapolitanus* to the Gram-positive soil bacterium *Corynebacterium glutamicum*. This member of the actinobacteria is used for the large-scale industrial production of amino acids and proteins (Eggeling and Bott, 2005; Wendisch, 2014). Metabolic engineering revealed its strong potential for the production of a variety of further value-added compounds including organic acids, polymer building blocks or plant natural products (Eggeling and Bott, 2015; Heider and Wendisch, 2015; Kallscheuer et al., 2016; Wendisch, 2014). Expression and presumably correct assembly of carboxysomes in *C. glutamicum* was demonstrated by purification of the microcompartments and identification of carboxysomal proteins by mass spectrometry. Different microscopy techniques and the measurement of RuBisCO activity provided further hints for the functionality of these compartments. This study provides important groundwork for the use of modular BMCs in bioengineering approaches for the improvement of small molecule production.

2. Materials and Methods

2.1 Bacterial strains, plasmids and growth conditions

All bacterial strains used in this study are listed in Table 1. *E. coli* DH5α and Stellar™ were used for cloning procedures and cultivated at 37°C in lysogeny broth (LB, (Sambrook and Russell, 2001)). *E. coli* DH5α was also used as a reference strain for carboxysome production. *C. glutamicum* ATCC 13032 was used as wild type and all derivatives thereof were constructed as indicated in Table 1. *C. glutamicum* was cultivated either in brain heart infusion broth (BHI, Difco Laboratories, Detroit, MI, USA) or in CGXII minimal medium (Keilhauer et al., 1993) supplemented with 3,4-dihydroxybenzoate (30 mg/l) as iron chelator and 2% (w/v) glucose as carbon source. As appropriate, kanamycin (50 µg/ml for *E. coli* or 25 µg/ml for *C. glutamicum)* and/or chloramphenicol (34 µg/ml for *E. coli* or 10 µg/ml for *C. glutamicum*) were added to the medium. Chromosomal DNA of *H. neapolitanus* was obtained from the DSMZ and used as PCR template. For the growth experiment a colony from a fresh agar plate was used to inoculate the preculture of 20 ml BHI in baffled shake flasks. The preculture was incubated at 30°C and 120 rpm overnight. On the following day the cells were washed twice with phosphate buffered saline (PBS) (137 mM NaCl, 2.7 mM KCl, 4.3 mM Na_2HPO_4, and 1.4 mM KH_2PO_4, pH 7.3) and used to inoculate the 750 µl main cultures to a starting OD_{600} of 1. The main cultivation was performed in 48-well flower plates (m2p labs, Baesweiler, Germany) in a BioLector microbioreactor system (m2p labs) at 30°C and 1200 rpm.

2.2 Recombinant DNA work and construction of chromosomal insertion strains

Routine methods such as PCR, DNA restriction and ligation were performed using standard protocols (Hanahan, 1983; Sambrook and Russell, 2001; van der Rest et al., 1999). The oligonucleotides used in this study were obtained from Eurofins Genomics (Ebersberg, Germany) and are listed in Table S1. The QIAquick Gel Extraction Kit, or the MinElute Gel

Extraction Kit (both Qiagen, Hilden, Germany) were used for gel purification of digested plasmids and PCR fragments, respectively. The In-Fusion ® HD Cloning Kit was obtained from Clontech Laboratories (Mountain View, Ca, USA) and used according to the manufacturer's instructions. All plasmid sequences were confirmed by sequencing (Eurofins Genomics, Ebersberg, Germany). Details about plasmid constructions are provided in the supplemental material (Text S1). Integration of carboxysomal gene clusters into the chromosome of *C. glutamicum* was performed by double-crossover as described previously (Baumgart et al., 2013).

2.3 Cell cultivation for carboxysome purification

For carboxysome purification 50 ml BHI with kanamycin in a baffled shake flask were inoculated with a single colony from a fresh transformation of ATCC 13032 carrying pAN6-HNC and cultivated at 30°C and 120 rpm overnight. For the main culture, 500 ml BHI with kanamycin in a baffled shake flask were inoculated with 20 ml of the preculture and cultivated at 30°C and 100 rpm. After 1.5 h the production of the carboxysomes was induced with 0.5 mM Isopropyl β-D-1-thiogalactopyranoside (IPTG) and the cells were further cultivated at 20°C until they were harvested on the following morning. The co-purification experiment was performed with the same cultivation procedure but chloramphenicol was added additionally to the medium as the strains were carrying two plasmids. For production of carboxysomes in *E. coli* 50 ml LB with kanamycin in a baffled shake flask were inoculated with a single colony of a fresh transformation of DH5α carrying pAN6-HNC and cultivated at 37°C and 120 rpm overnight. The main culture (500 ml LB with kanamycin in a baffled shake flask) was inoculated with 20 ml of the preculture and cultivated at 37°C and 100 rpm. At an OD_{600} of 0.5 the production of the carboxysomes was induced with 50 µM IPTG. The cells were further cultivated at 20°C until they were harvested on the following morning.

2.4 Purification of carboxysomes by sucrose gradient centrifugation

In principle, the carboxysome purification was performed as described previously (So et al., 2004), except for some adaptations to *C. glutamicum*. The cells of 1l of *C. glutamicum* cell culture expressing carboxysomes were harvested and washed once with PBS. The pellet was suspended in 25 ml TEMB (5 mM Tris-HCl pH 8.0, 1 mM EDTA, 10 mM $MgCl_2$, 20 mM $NaHCO_3$). Phenylmethylsulfonyl fluoride **(**PMSF, 0.5 mM final concentration) and Lysozyme (1 mg/ml final concentration) were added and the cell suspension was incubated slightly tilting for 1 h at room temperature. The cells were harvested and the supernatant was discarded. The pellet was suspended again in 25 ml TEMB containing 0.5 mM PMSF, 5 mM $CaCl_2$ and 50 µg/ml DNAseI. The cells were disrupted by passing five times through a French pressure cell at 15.000 psi. Subsequently, the suspension was further treated 1x1 min and 4x30 sec with two minutes of cooling in between with a Branson Sonifier 250 (Duty Cycle 40 %, Output Control 1). Cell debris and intact cells were separated by centrifugation at 4300*g* for 15 min at 4°C. The solution was further clarified by centrifugation in a JA-25.50 rotor at 12,096*g* and 4°C for 20 min. The supernatant was subsequently centrifuged at 45,000*g* and 4°C for 40 min to sediment the carboxysomes and membranes. The supernatant was discarded and the pellet resuspended in 5 ml TEMB with BugBuster™ (Novagen) and centrifuged again for 40 min at 4°C and 57,000*g*. The pellet was then resuspended in a small volume (≤ 1.5 ml) TEMB and centrifuged at 1000*g* for 3 min. The supernatant was subsequently loaded onto a sucrose gradient that had been prepared as following. Sucrose stock solutions with 10%, 20%, 30%, 40%, and 50% (w/v) sucrose in TEMB were prepared and cooled to 4°C. The gradients were prepared in 16x102mm polyallomer centrifuge tubes by adding first 3 ml of the 10% sucrose solution. This layer was sublayered with 3 ml of each of the other solutions with increasing sucrose concentrations using a syringe with a long cannula. In order to get a continuous gradient, the tubes were stored overnight at 4°C in an upright position. The gradient with the carboxysome solution on top was centrifuged for 40 min at 4 °C and

150,000*g* in a SW-28.1 rotor to separate the carboxysomes from soluble proteins and remaining cell debris. The gradient was fractionated by taking 1 ml fractions from the top using a pipette. The fractions were analyzed by SDS-PAGE, carboxysome containing fractions were pooled, diluted with TEMB to reduce the sucrose content of the sample and centrifuged for 90 min at 100,000*g* and 4°C to collect the purified carboxysomes. MALDI-TOF mass spectrometry of carboxysomal proteins was performed as described previously (Koch-Koerfges et al., 2012).

2.5 RuBisCO enzyme assay

The precultures were prepared as described for the purification of the carboxysomes. The 50 ml CGXII main cultures were inoculated with 2 ml preculture. After 24 h, the cells were harvested and 25 mL of the cultures were resuspended in 1 mL EME buffer (100 mM EPPS-NaOH, pH 8.2; 10 mM $MgCl_2$; 1 mM EDTA). The cell lysis was done by 3x 20 s intervalls at 6000 rpm in a Precellys® 24 homogeniser (Bertin instruments, Montigny-le-Bretonneux, France) and the crude extract was obtained by separating cell debris with a centrifugation step at 12,000*g* for 10 min at 4°C. The activity of RuBisCO was measured in crude extract using a spectrophotometric assay similar as described in (Kubien et al., 2011). In this assay, the RuBisCO reaction yielding 3-phosphoglycerate (3-PGA) is coupled with 3-PGA kinase (phosphorylates 3-PGA to 1,3 bisphosphoglycerate (1,3-BPG) with ATP) and glyceraldehyde 3-phosphate dehydrogenase (GAP-DH, reduces 1,3-BPG to glyceraldehyde 3-phosphate (GA3P) with NADH). For each carboxylated molecule of ribulose-1,5-bisphosphate (RuBP), two molecules of NADH are oxidized which can be followed at 340 nm. All enzymes were purchased from Sigma-Aldrich (Munich, Germany). First, an enzyme-mix stock solution was prepared. 2,500 U of 3-PGA kinase (supplied as $(NH_4)_2SO_4$ suspension) were transferred into a reaction tube and centrifuged (10,000*g*, 4°C, 20 min). The supernatant was discarded and the pellet resuspended in 1.5 ml EED-buffer (50 mM EPPS-NaOH, pH 7.8; 1 mM EDTA; 1

mM DTT (freshly prepared)). 2,500 U of Creatine-phosphate kinase, 25,000 U of carbonic anhydrase as well as 2,500 U of GAP-DH were added and the solution was dialyzed (2 x 2h and 1x overnight) at 4°C against EDD buffer. Afterwards the solution was centrifuged as above and the supernatant supplemented with glycerol to a final concentration of 20% (v/v). Aliquots were flash-frozen in liquid nitrogen and stored at -80°C until used for the assay. The assay reaction contained 200 µM NADH, 10 µM $NaHCO_3$, 1 mM ATP, 5 mM phosphocreatine, 1/50 volume enzyme mix stock solution and 500 µM RubBP in EME buffer. All stock solutions were prepared in EME buffer. The measurements were performed in an Amersham Ultrospec 2100 pro spectrophotometer at 30 °C and the reaction was started with RuBP. The disappearance of NADH (ε = 6200 l $mol^{-1} \cdot cm^{-1}$) was measured at 340 nm in an Amersham Ultrospec 2100 pro spectrophotometer at 30 °C. Before the addition of 10 µL RuBP, the background activity of 10 µL of each undiluted cell lysate in 480 µL assay solution was recorded for 1 minute. The actual reaction was monitored for 4 minutes after RuBP addition. One unit (U) of RuBisCO activity is defined as 1 µmol min^{-1} mg^{-1}.

2.6 Western blotting

The cells were cultivated as described for the carboxysome purification and disrupted with glass beads. The protein content of the crude cell extracts was measured with the Pierce™ BCA Protein Assay Kit (Thermo Fisher Scientific, Waltham, USA). Bovine serum albumine was used as protein standard. SDS-PAGE was performed with 4–20% Mini-PROTEAN® TGX™ Precast Protein Gels for detection of CbbL in RuBisCO assay samples and 10 % Tris/glycine handcast gels for the detection of CbbL-eYFP after copurification with carboxysomes. The samples were transferred onto a nitrocellulose membrane and probed with antibodies. As primary antibodies, Anti-RbcL (Agrisera, Vännas, Sweden) and Anti-GFP (ab290, Abcam, Cambridge, UK) were used. The alkaline phosphatase conjugated anti-Rabbit secondary antibody (GE Healthcare, Munich, Germany) was detected using a ECL™ Select

Western Blotting Detection Reagent (GE Healthcare) following the manufacturer‘s instructions.

2.7 Transmission electron microscopy (TEM)

For the analysis of cells expressing carboxysomes by TEM, samples were prepared as following. The cells were cultivated as described for the carboxysome purification procedure. *C. glutamicum* was harvested after overnight cultivation and *E. coli* 4 h after induction. 1 ml cell suspension was centrifuged for 1 min at 16,000*g* and the supernatant was discarded. The bacteria were resuspended in 1 ml PBS and fixed with 3% (v/v) glutaraldehyde (Agar scientific, Wetzlar, Germany) in PBS for at least 4 h. Embedding in epon, staining with uranyl acetate as well as TEM picture collection was performed as described previously (Baumgart et al., 2016).

2.8 Fluorescence microscopy

For fluorescence microscopy, 5 ml BHI with the required antibiotics in a test tube were inoculated with a single colony from a fresh agar plate and incubated at 30°C and 170 rpm overnight. On the following day 100 µl of this preculture were used to inoculate the main culture, 5 ml CGXII-medium with the required antibiotics and 10 µM IPTG. The main culture was incubated at the same conditions as the preculture and cell samples were analyzed by fluorescence microscopy at different time points. The cells were analyzed on agarose pads using a Zeiss Axio Imager M2 microscope that was equipped with an AxioCam MRm camera and a Plan-Apochromat 100x, 1.40 Oil phase contrast oil-immersion objective. Digital images were acquired and analyzed with AxioVision 4.8 software (Zeiss, Göttingen, Germany).

3. Results & Discussion

3.1 Heterologous expression of carboxysomes in *C. glutamicum*

C. glutamicum ATCC 13032 is intensively engineered as platform for the production of a variety of value-added compounds in biotechnological processes (Eggeling and Bott, 2015; Heider and Wendisch, 2015). Therefore, the encapsulation of heterologous pathways might represent an elegant approach to minimize detrimental metabolic interactions within the cytoplasm and to enhance productivity. The genome sequences of published *C. glutamicum* strains do not reveal any obvious BMC clusters. Here, we set out to express and assemble functional carboxysomes in *C. glutamicum.* For this purpose, the carboxysome encoding operon of *H. neapolitanus* (Fig. 1A) was cloned into a *C. glutamicum* expression plasmid under control of the IPTG inducible P_{tac} promoter and expressed both in *C. glutamicum* as well as in *E. coli* as a heterologous reference strain where functional assembly was already shown in a previous study (Bonacci et al., 2012). Comparative phenotypical analyses revealed that *C. glutamicum* seems to tolerate the carboxysomes rather well and exhibited normal cell morphology (Figs. S1A and S1B), whereas the *E. coli* strain expressing the carboxysomal operon was growing very slowly even without induction and formed strongly elongated cells with inclusion bodies which are visible as refractive particles within the cell (Figs. S1C and S1D). This drastic impact on growth and cell morphology is in line with the previous work of Bonacci and coworkers who also reported the formation of inclusion bodies in *E. coli* upon stronger induction of the gene cluster (Bonacci et al., 2012).

Transmission electron microscopy (TEM) of *C. glutamicum* wild type cells revealed several intracellular structures which likely represent volutin granules composed of polyphosphate as reported in previous studies (Pallerla et al., 2005) (Figs. 1B and S2). Although these were usually roundish and larger than the expected carboxysomes they nevertheless hampered the clear identification of carboxysomes within cells by TEM. *C. glutamicum* cells expressing the

carboxysomal operon from a plasmid (pAN6-HNC or pAN6-HNC+CsoS1D) revealed BMC-like structures, some of which were of hexagonal shape (Figs. 1C and S3). Even in thin sections up to six carboxysome-like structures were visible. These structures were similar to the BMCs observed by Bonacci et al. in *E. coli* (Bonacci et al., 2012) but more irregularly shaped compared to the native host (So et al., 2004). Cells with the chromosomal carboxysome gene cluster showed only structures that looked very much alike those observed in the wild type (data not shown), probably due to rather low expression and a limited number of cells studied.

3.2 Purification of carboxysomes from *C. glutamicum* and *E. coli*

To test for the correct assembly of the carboxysomal components, carboxysomes were purified from *C. glutamicum* cells expressing the *H. neapolitanus* operon (Fig. 1A). In contrast to *E. coli*, the cell disruption of *C. glutamicum* represented a major challenge of the purification procedure because of the rigid cell wall architecture hampering cell disruption without destroying the carboxysomes. The final carboxysome yield was much lower compared to *E. coli*. Overall, the purification procedure included several centrifugation steps and is shown schematically in Fig. 2A (So et al., 2004). During the final sucrose gradient centrifugation soluble proteins (stay on top) as well as aggregated proteins and other impurities (sediment to the bottom) are separated from the carboxysomes, which are usually located approximately in the middle of the gradient. The fact, that carboxysomal proteins were identified in the gradient strongly suggested the formation of BMCs, as inclusion bodies and large aggregates would sediment under the applied conditions. (Upadhyay et al., 2012). SDS-PAGE revealed carboxysomal proteins in several fractions of the gradient (Fig. S4). The bands were subjected to MALDI-TOF analysis and all carboxysomal proteins except for CsoS4A and CsoS4B were identified in the *C. glutamicum* sample (Fig. 2B) confirming their expression and presumably the assembly of the carboxysomes.

297 Although the same plasmid was used for carboxysome production, the protein pattern differed
298 between the two expression hosts. In contrast to *E. coli* (Bonacci et al., 2012), CsoS3 was
299 identified in the *C. glutamicum* sample in two bands at the theoretical molecular weight of
300 about 57.3 kDa (Fig. 2B). While there were two prominent bands for CsoS2 in the *E. coli*
301 carboxysomes, there is only one major CsoS2 band in the *C. glutamicum* sample. The
302 appearance of CsoS2 in different bands has also been reported previously for carboxysomes
303 purified from *E. coli* (Bonacci et al., 2012) or the native host (Baker et al., 1999; So et al.,
304 2004). While it was first hypothesized that the two bands result from different
305 posttranslational modifications (Baker et al., 1999), it was recently proposed that the lower
306 band corresponds to a C-terminally truncated version of CsoS2 (Cai et al., 2015). The fact that
307 the lower CsoS2 band is hardly visible in the *C. glutamicum* carboxysome preparation
308 suggests that the processing of this protein is somehow different in *C. glutamicum* which may
309 also influence the size or shape of the carboxysomes in this species.

310 TEM analysis of carboxysomes purified from *C. glutamicum* and *E. coli* (Figs. 2C and 2D)
311 revealed that the microcompartments from *C. glutamicum* where much smaller than those
312 from *E. coli* and their shape appeared to be more round than hexagonal. The compartments
313 look different to previously published pictures of carboxysomes (Bonacci et al., 2012) but this
314 might be a result from the different preparation techniques used. Considering the differences
315 in cell wall architecture, larger BMCs of *C. glutamicum* might have become a victim of the
316 cell disruption protocol. Alternatively, differences in the processing and/or modification of
317 carboxysomal proteins (e.g. CsoS2, see above) might influence the BMC morphology. We
318 also tested the co-expression of the *csoS1D* gene which may be relevant for pore formation
319 and significantly improved the carboxysome quality in *E. coli* (Bonacci et al., 2012). But this
320 apparently did not stabilize the carboxysomes in *C. glutamicum* (data not shown). Overall, the

purification via the sucrose gradient adds a further piece of evidence for the successful assembly of heterologous carboxysomes in *C. glutamicum.*

3.3 Chromosomal integration of the carboxysomal gene cluster

In order to be independent of plasmid-based expression of carboxysomes in further studies, *C. glutamicum* strains with chromosomally integrated gene-clusters were constructed. Resulting strains contained either the whole carboxysome operon (Fig. 1A) or just the genes for the shell proteins under control of the constitutive promoter P_{tuf}. It has been reported that *H. neapolitanus* carboxysomal proteins are able to form empty microcompartments in the absence of the RuBisCO proteins CbbLS (Menon et al., 2008). Western blot analysis of crude cell extracts with anti-RbcL-antibodies showed that RuBisCO was expressed by the strains with the chromosomal or plasmid encoded native carboxysome operon (Fig. 3A). However, the RuBisCO amount was much lower compared to the plasmid based expression of only *cbbLS* upon induction (pAN6-HNcbbLS).

3.4 RuBisCO activity in carboxysome producing strains

The activity of RuBisCO was assayed in different strains to assess, whether the enzyme is produced in an active state in *C. glutamicum*. The crude extract of *C. glutamicum* carrying plasmid pAN6-HNcbbLS displayed an activity of 100.6 ± 11.2 mU/mg cell extract (Fig. 3B) confirming the functional production of the heterologous RuBisCO enzyme in *C. glutamicum.* In the strain expressing the whole carboxysome operon from a plasmid, the activity was 0.6 ± 0.4 mU/mg cell extract without induction and 14.3 ± 3.8 mU/mg cell extract after induction with IPTG. This activity is clearly above the background level (0.1 ± 0.1 mU/mg cell extract) and, thus, confirms the enzymatic activity of the RuBisCO when co-expressed with the other carboxysomal proteins. The strain carrying the chromosomal carboxysome operon shows a RuBisCO activity of 3.6 ± 1.4 mU/mg cell extract which is also significantly above

background. In all samples, the measured RuBisCO activity correlated well with the protein amount as demonstrated by Western blotting (Fig. 3A).

3.5 Influence of carboxysome expression on growth of *C. glutamicum*

In further experiments, the impact of carboxysome expression on growth was monitored. While the chromosomal integration had no significant effect on growth (Fig. 4A) there was a slight effect on growth when the carboxysomes were expressed from a plasmid, but the cells reached almost the same final backscatter compared to the empty plasmid control (Fig. 4B). For *E. coli* it was shown that the expression of carboxysomes rescues the growth defect of a strain expressing phosphoribulokinase (PRK) by counteracting the irreversible production of D-ribulose 1,5-bisphosphate, but this strain still growths worse than the wild type (Bonacci et al., 2012). Attempts to construct a *C. glutamicum* strain expressing *prkA* were extremely hindered already at the cloning stage by the high toxicity of PrkA in the absence of RuBisCO (data not shown).

3.6 Localization studies with carboxysomal proteins fused to fluorescent proteins

Fusion proteins of carboxysomal and fluorescent proteins have previously been used to analyze and visualize carboxysome formation in living cells (Bonacci et al., 2012; Savage et al., 2010). To further investigate the assembly of carboxysomes in *C. glutamicum*, several fusions of carboxysomal proteins to fluorescent proteins were constructed and analyzed in different strains by fluorescence microscopy. In a first attempt, the carboxysomal shell protein CsoS1A was fused C-terminally to CFP. In the wild type, CsoS1A-CFP was evenly distributed in the cell (Fig. 5A) which is in contrast to the distribution of CsoS1A-GFP in *E. coli* were this fusion protein was reported to form large polar aggregates even in the absence of any other carboxysomal protein (Bonacci et al., 2012). When the same construct was used in the carboxysome encoding strains, several foci appeared suggesting that the fusion protein was targeted to the carboxysomal shell (Fig. 5A). As control, *cfp* alone was expressed in the

strains expressing carboxysomal proteins and it was evenly distributed in all cases (data not shown). In *E. coli*, the co-expression of CsoS1A-GFP with carboxysomes did not abolish inclusion body formation but led to the appearance of faint, additional cytoplasmic foci (Bonacci et al., 2012). Similar results to CsoS1A-CFP were obtained for CsoS2-eYFP (Fig. 5B). This fusion was further analyzed by single molecule localization microscopy (SMLM), revealing fluorescent foci of different size and distribution (60 – 250 nm large) in about 40% of the cells (Text S1, Fig. S5, Table S2).

Constructs of *H. neapolitanus* carbonic anhydrase HNCA, CbbL and CbbS fused to eYFP already formed foci in the wild type without any additional carboxysomal proteins suggesting the formation of protein aggregates (Fig. S6 and data not shown). However, the amount of CbbS-eYFP foci was increased in the presence of the other carboxysomal proteins (strain ATCC 13032::HNC-whole; on average 1.34 foci per cell, n=179) in comparison to a strain lacking the operon (0.85 foci per cell, n=146).

In further experiments, CsoS1A-CFP was combined with CsoS2-eYFP, CbbL-eYFP or CbbS-eYFP within one cell to study their co-localization (Fig. 5C). In these experiments the proteins already formed some foci when co-expressed in the wild type, but the share of cells with foci was always increased when whole carboxysomes or just the shell proteins were present (Fig. S7). In the wildtype, about 20% co-localization was observed for the combination of CbbL-eYFP with CsoS1A-CFP but not for the other combinations (Fig. 5D). In the presence of carboxysomal proteins, the frequency of co-localization increased to 40-100% (Fig. 5D). Taking these results together, we could show that the presence of carboxysomal proteins significantly increased the frequency of foci formation of fusion proteins that are evenly distributed when expressed alone (CsoS1A-CFP and CsoS2-eYFP). Furthermore, the production of carboxysomal proteins enforced the co-localization of different carboxysomal proteins. However, in several cells the appearance of large polar

structures was observed suggesting the formation of protein aggregates in cells expressing the carboxysomal gene cluster. Therefore, further attempts described in the following paragraph focused on the optimization of the expression level.

3.7 Impact of induction level on carboxysome formation

Previous studies in *E. coli* showed that the best carboxysome formation was observed at low or medium induction levels (Bonacci et al., 2012). To study the influence of induction on carboxysome formation in *C. glutamicum* we constructed a plasmid containing a *csoS1A-eyfp* fusion under control of a constitutive promoter (P_{acn}, promoter of the *C. glutamicum* aconitase gene). This plasmid was used to transform ATCC 13032::HNC-whole carrying the chromosomal carboxysome operon under control of a constitutive promoter as well as strain ATCC 13032 carrying the plasmid encoded and inducible carboxysome operon (pAN6-HNC). This setup allowed analyzing the impact of the expression level of the carboxysomal gene cluster on carboxysome formation while the amount of CsoS1A-eYFP was kept constant. Whereas in cells with low induction level or chromosomally encoded carboxysomes only a few fluorescent foci (0-2) were observed. Induction of ATCC 13032 pAN6-HNC correlated with an increase of fluorescent foci in number and size over time (Fig. 6 and Fig. S8). Here, the appearance of larger foci at high induction levels likely reveals the appearance of protein aggregates. Upon high induction levels, cells typically elongated showing the formation of intracellular inclusion bodies visible as refractive particles in the phase contrast. Imaging of stationary cells (at 25 h) indicated the formation of aggregated CsoS1A-eYFP protein, which was evenly distributed in the exponential phase (Fig. S9). Therefore, we focused on the analysis of different induction levels on carboxysomes formation in exponentially growing cells.

3.8 Co-purification of CbbL-eYFP with carboxysomes

For the use of microcompartments as nano-bioreactors it is essential to incorporate enzymes of interest into the carboxysomal shells. Early studies proposed that the shell forms first ad RuBisCO is subsequently transported into the carboxysomes (Price and Badger, 1991). However, more recent results argue against this model and suggest that shell assembly and RuBisCO happens simultaneously and is more likely driven by protein-protein interactions than by special signal sequences (Iancu et al., 2010). To further investigate whether proteins fused to carboxysomal proteins are targeted to our carboxysomes, we tested whether CbbL-eYFP can be purified together with whole carboxysomes. As control, a strain expressing the carboxysome operon and *eyfp* alone was used. Carboxysomes were purified as described above and samples of the sucrose gradient were probed with antibodies against eYFP or CbbL. While the amount of carboxysomes purified from both samples was very similar, only the sample of the strain expressing the fusion protein displayed a band of about 80 kDa corresponding to the molecular weight of CbbL-eYFP (Fig. 7). These data suggest that proteins fused to CbbL were targeted to the heterologous BMCs.

4. Conclusion

Carboxysomes represent the currently best-studied proteinaceous bacterial microcompartments. Their overall modularity provoked strong interests for application in synthetic biology, most importantly for the encapsulation and scaffolding of heterologous pathways. The potential use of carboxysomes as nano-bioreactors for biotechnological application requires a detailed knowledge of the assembly and cell biology in their native hosts. Regarding the heterologous production of bacterial microcompartments, all studies so far focused on *E. coli* (Bonacci et al., 2012), with one exception where β-carboxysomes were introduced into chloroplasts of the plant *Nicotiana benthamiana* (Lin et al., 2014). Several recent studies report on the modular character of BMC and their potential for improving the

performance of synthetic metabolic pathways. However, an implementation into metabolic engineering approaches demands for the successful assembly of BMC shells within the particular host system. With this study, we highlight several challenges affecting the transfer and heterologous establishment of BMCs into a well-characterized model organism such as *C. glutamicum*. Notably, the expression of carboxysomal gene clusters slightly affected cell morphology and growth but this effect is less severe than the effect caused by the expression of the same gene cluster in *E. coli*. However, a strong piece of evidence for the assembly of BMC-like structures – at least in some of the cells - is the presence of almost all carboxysomal proteins in the middle of the sucrose gradient. Furthermore, we observed significant differences when comparing the two model strains *E. coli* and *C. glutamicum* in terms of the overall cell morphology and growth as well as in processing/modification of carboxysomal shell proteins (e.g. differences in the band pattern for CsoS2). In *E. coli*, the additional expression of the phosphoribulokinase gene (*prkA*) enabled the establishment of a synthetic carbon fixing organelle (Bonacci et al., 2012). However, our attempts in *C. glutamicum* revealed significant challenges already at the cloning stage due to the high toxicity of the *prkA* gene (data not shown). Obviously, the successful production of synthetic microcompartments depends on extensive adaption to achieve optimal functionality in the particular host system. Optimization of BMC assembly and functionality will include balancing of the stoichiometry of BMC proteins, consideration of interactions with the cytoskeleton, additional assembly factors and efficient targeting of cargo proteins into the BMC lumen (Cheng et al., 2012; Parsons et al., 2010; Rae et al., 2012). Consequently, further studies are required for benchmarking the potential value of synthetic BMCs for biotechnological production by weighing the pros and cons for the particular process.

Authors' contributions

MB designed all experiments and performed the experiments including cloning, strain construction, carboxysome purification, TEM, and fluorescence microscopy and analyzed the data. IH performed the RuBisCO activity assays, Western Blotting and parts of the fluorescence microscopy studies and analyzed the corresponding data. IA and TG performed the SMLM and analyzed the corresponding data. MB and JF conceived of the study and wrote the manuscript. All approved the final manuscript.

Acknowledgements

We thank Mareike Hoß and Hiltrud Königs from the electron microscopy department of the UK Aachen for TEM pictures and Cornelia Gätgens as well as Christina Mack for great technical support.

Funding

This work was supported by the Helmholtz association (grant VH-NG-716) and the federal ministry of education and research (grant 0316017B).

References

Alm, E.J., Huang, K.H., Price, M.N., Koche, R.P., Keller, K., Dubchak, I.L., Arkin, A.P., (2005) The MicrobesOnline Web site for comparative genomics. Genome Res. 15, 1015-1022.

Axen, S.D., Erbilgin, O., Kerfeld, C.A., (2014) A taxonomy of bacterial microcompartment loci constructed by a novel scoring method. PLoS Comput. Biol. 10, e1003898.

Badger, M.R., Price, G.D., (2003) CO_2 concentrating mechanisms in cyanobacteria: molecular components, their diversity and evolution. J. Exp. Bot. 54, 609-622.

Baker, S.H., Jin, S., Aldrich, H.C., Howard, G.T., Shively, J.M., (1998) Insertion mutation of the form I *cbbL* gene encoding ribulose bisphosphate carboxylase/oxygenase (RuBisCO) in *Thiobacillus neapolitanus* results in expression of form II RuBisCO, loss of carboxysomes, and an increased CO_2 requirement for growth. J. Bacteriol. 180, 4133-4139.

Baker, S.H., Lorbach, S.C., Rodriguez-Buey, M., Williams, D.S., Aldrich, H.C., Shively, J.M., (1999) The correlation of the gene *csoS2* of the carboxysome operon with two polypeptides of the carboxysome in *Thiobacillus neapolitanus*. Arch. Microbiol. 172, 233-239.

Baumgart, M., Schubert, K., Bramkamp, M., Frunzke, J., (2016) Impact of LytR-CpsA-Psr proteins on cell wall biosynthesis in *Corynebacterium glutamicum*. J. Bacteriol. 198, 3045-3059.

Baumgart, M., Unthan, S., Rückert, C., Sivalingam, J., Grünberger, A., Kalinowski, J., Bott, M., Noack, S., Frunzke, J., (2013) Construction of a prophage-free variant of *Corynebacterium glutamicum* ATCC 13032 for use as a platform strain for basic research and industrial biotechnology. Appl. Environ. Microbiol. 79, 6006-6015.

Bobik, T.A., Lehman, B.P., Yeates, T.O., (2015) Bacterial microcompartments: widespread prokaryotic organelles for isolation and optimization of metabolic pathways. Mol. Microbiol. 98, 193-207.

Bonacci, W., Teng, P.K., Afonso, B., Niederholtmeyer, H., Grob, P., Silver, P.A., Savage, D.F., (2012) Modularity of a carbon-fixing protein organelle. Proc. Natl. Acad. Sci. USA 109, 478-483.

Cai, F., Dou, Z., Bernstein, S.L., Leverenz, R., Williams, E.B., Heinhorst, S., Shively, J., Cannon, G.C., Kerfeld, C.A., (2015) Advances in understanding carboxysome assembly in *Prochlorococcus* and *Synechococcus* implicate CsoS2 as a critical component. Life (Basel) 5, 1141-1171.

Cameron, J.C., Wilson, S.C., Bernstein, S.L., Kerfeld, C.A., (2013) Biogenesis of a bacterial organelle: the carboxysome assembly pathway. Cell 155, 1131-1140.

Cheng, S., Fan, C., Sinha, S., Bobik, T.A., (2012) The PduQ enzyme is an alcohol dehydrogenase used to recycle NAD^+ internally within the Pdu microcompartment of *Salmonella enterica*. PLoS One 7, e47144.

Choudhary, S., Quin, M.B., Sanders, M.A., Johnson, E.T., Schmidt-Dannert, C., (2012) Engineered protein nano-compartments for targeted enzyme localization. PLoS One 7, e33342.

Chowdhury, C., Sinha, S., Chun, S., Yeates, T.O., Bobik, T.A., (2014) Diverse bacterial microcompartment organelles. Microbiol. Mol. Biol. Rev. 78, 438-468.

Eggeling, L., Bott, M., (2005) Handbook of *Corynebacterium glutamicum*. CRC Press, Taylor & Francis Group, Boca Raton, Florida, USA.

Eggeling, L., Bott, M., (2015) A giant market and a powerful metabolism: L-lysine provided by *Corynebacterium glutamicum*. Appl. Microbiol. Biotechnol. 99, 3387-3394.

Eikmanns, B.J., Kleinertz, E., Liebl, W., Sahm, H., (1991) A family of *Corynebacterium glutamicum*/*Escherichia coli* shuttle vectors for cloning, controlled gene expression, and promoter probing. Gene 102, 93-98.

Frank, S., Lawrence, A.D., Prentice, M.B., Warren, M.J., (2013) Bacterial microcompartments moving into a synthetic biological world. J. Biotechnol. 163, 273-279.
Frunzke, J., Engels, V., Hasenbein, S., Gätgens, C., Bott, M., (2008) Co-ordinated regulation of gluconate catabolism and glucose uptake in *Corynebacterium glutamicum* by two functionally equivalent transcriptional regulators, GntR1 and GntR2. Mol. Microbiol. 67, 305-322.
Gupta, R.S., (2012) Origin and spread of photosynthesis based upon conserved sequence features in key bacteriochlorophyll biosynthesis proteins. Mol. Biol. Evol. 29, 3397-3412.
Hanahan, D., (1983) Studies on transformation of *Escherichia coli* with plasmids. J. Mol. Biol. 166, 557-580.
Heider, S.A., Wendisch, V.F., (2015) Engineering microbial cell factories: Metabolic engineering of *Corynebacterium glutamicum* with a focus on non-natural products. Biotechnol. J. 10, 1170-1184.
Hentschel, E., Will, C., Mustafi, N., Burkovski, A., Rehm, N., Frunzke, J., (2013) Destabilized eYFP variants for dynamic gene expression studies in *Corynebacterium glutamicum*. Microb. Biotechnol. 6, 196-201.
Iancu, C.V., Morris, D.M., Dou, Z., Heinhorst, S., Cannon, G.C., Jensen, G.J., (2010) Organization, structure, and assembly of α-carboxysomes determined by electron cryotomography of intact cells. J. Mol. Biol. 396, 105-117.
Kallscheuer, N., Vogt, M., Stenzel, A., Gätgens, J., Bott, M., Marienhagen, J., (2016) Construction of a *Corynebacterium glutamicum* platform strain for the production of stilbenes and (2S)-flavanones. Metab. Eng. 38, 47-55.
Kaneko, Y., Danev, R., Nagayama, K., Nakamoto, H., (2006) Intact carboxysomes in a cyanobacterial cell visualized by hilbert differential contrast transmission electron microscopy. J. Bacteriol. 188, 805-808.
Keilhauer, C., Eggeling, L., Sahm, H., (1993) Isoleucine synthesis in *Corynebacterium glutamicum* - Molecular analysis of the *IlvB-IlvN-IlvC* operon. J. Bacteriol. 175, 5595-5603.
Kelly, D.P., Wood, A.P., (2000) Reclassification of some species of *Thiobacillus* to the newly designated genera *Acidithiobacillus* gen. nov., *Halothiobacillus* gen. nov. and *Thermithiobacillus* gen. nov. Int. J. Syst. Evol. Microbiol. 50 Pt 2, 511-516.
Kerfeld, C.A., Erbilgin, O., (2015) Bacterial microcompartments and the modular construction of microbial metabolism. Trends Microbiol. 23, 22-34.
Kerfeld, C.A., Melnicki, M.R., (2016) Assembly, function and evolution of cyanobacterial carboxysomes. Curr. Opin. Plant Biol. 31, 66-75.
Kinney, J.N., Salmeen, A., Cai, F., Kerfeld, C.A., (2012) Elucidating essential role of conserved carboxysomal protein CcmN reveals common feature of bacterial microcompartment assembly. J. Biol. Chem. 287, 17729-17736.
Kinoshita, S., Udaka, S., Shimono, M., (1957) Studies of amino acid fermentation. I. Production of L-glutamic acid by various microorganisms. J. Gen. Appl. Microbiol. 3, 193-205.
Kirchner, O., Tauch, A., (2003) Tools for genetic engineering in the amino acid-producing bacterium *Corynebacterium glutamicum*. J. Biotechnol. 104, 287-299.
Koch-Koerfges, A., Kabus, A., Ochrombel, I., Marin, K., Bott, M., (2012) Physiology and global gene expression of a *Corynebacterium glutamicum* ΔF_1F_O-ATP synthase mutant devoid of oxidative phosphorylation. Biochim. Biophys. Acta 1817, 370-380.
Kubien, D.S., Brown, C.M., Kane, H.J., (2011) Quantifying the amount and activity of Rubisco in leaves. Methods Mol. Biol. 684, 349-362.
Lin, M.T., Occhialini, A., Andralojc, P.J., Devonshire, J., Hines, K.M., Parry, M.A., Hanson, M.R., (2014) β-Carboxysomal proteins assemble into highly organized structures in *Nicotiana* chloroplasts. Plant J. 79, 1-12.

Menon, B.B., Dou, Z., Heinhorst, S., Shively, J.M., Cannon, G.C., (2008) *Halothiobacillus neapolitanus* carboxysomes sequester heterologous and chimeric RubisCO species. PLoS One 3, e3570.
Pallerla, S.R., Knebel, S., Polen, T., Klauth, P., Hollender, J., Wendisch, V.F., Schoberth, S.M., (2005) Formation of volutin granules in *Corynebacterium glutamicum*. FEMS Microbiol. Lett. 243, 133-140.
Parsons, J.B., Dinesh, S.D., Deery, E., Leech, H.K., Brindley, A.A., Heldt, D., Frank, S., Smales, C.M., Lunsdorf, H., Rambach, A., Gass, M.H., Bleloch, A., McClean, K.J., Munro, A.W., Rigby, S.E., Warren, M.J., Prentice, M.B., (2008) Biochemical and structural insights into bacterial organelle form and biogenesis. J. Biol. Chem. 283, 14366-14375.
Parsons, J.B., Frank, S., Bhella, D., Liang, M., Prentice, M.B., Mulvihill, D.P., Warren, M.J., (2010) Synthesis of empty bacterial microcompartments, directed organelle protein incorporation, and evidence of filament-associated organelle movement. Mol. Cell 38, 305-315.
Price, G.D., Badger, M.R., (1991) Evidence for the role of carboxysomes in the cyanobacterial CO_2-concentrating mechanism. Canadian Journal of Botany 69, 963-973.
Rae, B.D., Long, B.M., Badger, M.R., Price, G.D., (2012) Structural determinants of the outer shell of β-carboxysomes in *Synechococcus elongatus* PCC 7942: roles for CcmK2, K3-K4, CcmO, and CcmL. PLoS One 7, e43871.
Rae, B.D., Long, B.M., Badger, M.R., Price, G.D., (2013) Functions, compositions, and evolution of the two types of carboxysomes: polyhedral microcompartments that facilitate CO_2 fixation in cyanobacteria and some proteobacteria. Microbiol. Mol. Biol. Rev. 77, 357-379.
Sambrook, J., Russell, D.W., (2001) Molecular cloning: A laboratory manual, 3rd ed. Cold Spring Harbor Laboratory Press, NY.
Savage, D.F., Afonso, B., Chen, A.H., Silver, P.A., (2010) Spatially ordered dynamics of the bacterial carbon fixation machinery. Science 327, 1258-1261.
So, A.K.C., Espie, G.S., Williams, E.B., Shively, J.M., Heinhorst, S., Cannon, G.C., (2004) A novel evolutionary lineage of carbonic anhydrase (ε class) is a component of the carboxysome shell. J. Bacteriol. 186, 623-630.
Upadhyay, A.K., Murmu, A., Singh, A., Panda, A.K., (2012) Kinetics of inclusion body formation and its correlation with the characteristics of protein aggregates in *Escherichia coli*. PLoS One 7, e33951.
van der Rest, M.E., Lange, C., Molenaar, D., (1999) A heat shock following electroporation induces highly efficient transformation of *Corynebacterium glutamicum* with xenogeneic plasmid DNA. Appl. Microbiol. Biotechnol. 52, 541-545.
Wendisch, V.F., (2014) Microbial production of amino acids and derived chemicals: synthetic biology approaches to strain development. Curr. Opin. Biotechnol. 30, 51-58.

Tables

Table 1

Bacterial strains and plasmids used in this study.

Strain or plasmid	Relevant characteristics	Source or Reference
E. coli		
DH5α	F⁻ *endA1* Φ80d*lacZ*ΔM15 Δ(*lacZYA-argF*)U169 *recA1 relA1 hsdR17*($r_K^-m_K^+$) *deoR supE44 thi-1 gyrA96 phoA* λ⁻; strain used for general cloning procedures and carboxysome expression	(Hanahan, 1983)
Stellar™	F⁻ *endA1* Φ80d*lacZ*ΔM15 Δ(*lacZYA-argF*)U169 *recA1 relA1 supE44 thi-1 gyrA96 phoA* Δ(*mrr-hsd*RMS-*mcr*BC) Δ*mcrA* λ⁻; strain used for InFusion cloning	Clontech Laboratories
C. glutamicum		
ATCC 13032	Biotin-auxotrophic wild type	(Kinoshita et al., 1957)
ATCC 13032::HNC-whole	Derivative of ATCC 13032 with a chromosomal insertion of the carboxysomal gene cluster under control of P_{tuf} between cg1121 and cg1122.	This work
ATCC 13032::HNC-shell	Derivative of ATCC 13032 with a chromosomal insertion of the carboxysomal shell gene cluster under control of P_{tuf} between cg1121 and cg1122.	This work
H. neapolitanus		
DSM 15147	Wildtype, DNA obtained from the DSMZ	(Kelly and Wood, 2000)
Plasmids		
pAN6	Kan^R; *C. glutamicum*/*E. coli* shuttle plasmid for regulated gene expression using P_{tac} (P_{tac} *lacI*^{q} pBL1 *ori*V_{Cg} pUC18 *ori*V_{Ec})	(Frunzke et al., 2008)
pAN6-HNC	Kan^R, derivative of pAN6 containing the *H. neapolitanus* carboxysome gene cluster	This work
pAN6-HNC-shell	Kan^R, derivative of pAN6 containing the *H. neapolitanus* carboxysome gene cluster without the genes for RuBisCO and carbonic anhydrase	This work
pAN6-HNC+CsoS1D	Kan^R, derivative of pAN6-HNC with additional *csoS1D* of *H. neapolitanus*	This work
pAN6-HNcbbLS	Kan^R, derivative of pAN6 containing the *H. neapolitanus* RuBisCO	This work
pK18-*mobsacB*-int1	Kan^R; plasmid for integration of foreign DNA into the intergenic region between cg1121-cg1122 (*ori*$V_{E.c.}$, *sacB*, *lacZ*α)	(Baumgart et al., 2013)

pK18-HNC-int	Kan^R, derivative of pK18-int1 for the chromosomal integration of the whole *H. neapolitanus* carboxysome gene cluster under control of P_{tuf}	This work
pK18-HNC-shell-int	Kan^R, derivative of pK18-int1 for the chromosomal integration of the *H. neapolitanus* carboxysomal shell gene cluster under control of P_{tuf}	This work
pEC-XC99E	Cm^R; *C. glutamicum*/*E. coli* shuttle plasmid for regulated gene expression using P_{trc}(P_{trc} *lacI*^{q} pGA1 *ori*V_{Cg}, *ori*V_{Ec})	(Kirchner and Tauch, 2003)
pEC-eYFP	Cm^R, derivative of pEC-XC99E containing *eyfp* with artificial RBS, under control of P_{trc}	This work
pEC-HNcbbL-eYFP	Cm^R; derivative of pEC-XC99E, contains the coding sequence of *H. neapolitanus cbbL* with RBS fused C-terminally to *eyfp*	This work
pEC-cbbS-eYFP	Cm^R; derivative of pEC-XC99E, contains the coding sequence of *H. neapolitanus cbbS* with RBS fused C-terminally to *eyfp*	This work
pEC-HNCA-eYFP	Cm^R; derivative of pEC-XC99E, contains the coding sequence of *H. neapolitanus CsoS3* (carbonic anhydrase) with RBS fused C-terminally to *eyfp*	This work
pEC-CsoS2-eYFP	Cm^R; derivative of pEC-XC99E, contains the coding sequence of *H. neapolitanus csoS2* with RBS fused C-terminally to *eyfp* under control of the constitutive *C glutamicum* aconitase promoter P_{acn}.	This work
pEC-Pacn-CsoS1A-eYFP	Cm^R; derivative of pEC-XC99E, contains the coding sequence of *H. neapolitanus csoS1A* with RBS fused C-terminally to *eyfp*	This work
pEKEx2	Kan^R; *C. glutamicum*/*E. coli* shuttle vector for regulated gene expression using P_{tac} (P_{tac} *lacI*^{q} pBL1 *ori*V_{Cg} pUC18 *ori*V_{Ec})	(Eikmanns et al., 1991)
pEKEx2-*eyfp*	Kan^R, pEKEx2 containing *eyfp* with artificial RBS, under control of P_{tac}	(Hentschel et al., 2013)
pEKEx2-CFP	Kan^R; derivative of pEKEx2, contains the *cfp* coding sequence with RBS	This work
pEKEx2-CsoS1A-CFP	Kan^R; derivative of pEKEx2, contains the coding sequence of *H. neapolitanus csoS1A* with RBS fused C-terminally to *cfp*	This work

623

624

Figure legends

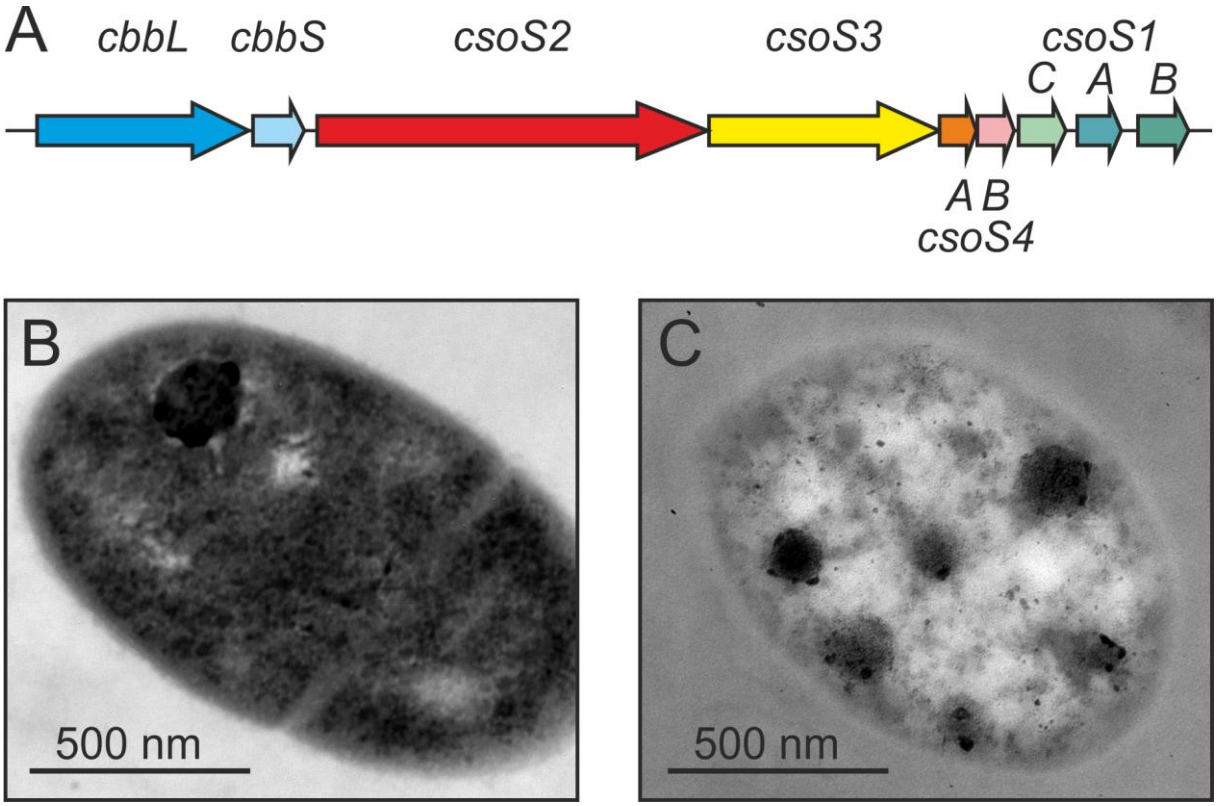

Fig. 1. Heterologous expression of carboxysomes in *C. glutamicum*. The carboxysome gene cluster of *H. neapolitanus* (A) with *cbbLS* encoding the large and the small subunit of the RuBisCO enzyme and *csoS3* encoding carbonic anhydrase. *csoS1CAB, csoS2* as well as *csoS4AB* encode shell proteins. The genes correspond to Hneap_0922 to Hneap_0914, data taken from (Alm et al., 2005). (B) and (C), TEM pictures of *C. glutamicum* wild type (B) and *C. glutamicum* expressing carboxysomes from plasmid pAN6-HNC (C) at a magnification of ×46,000.

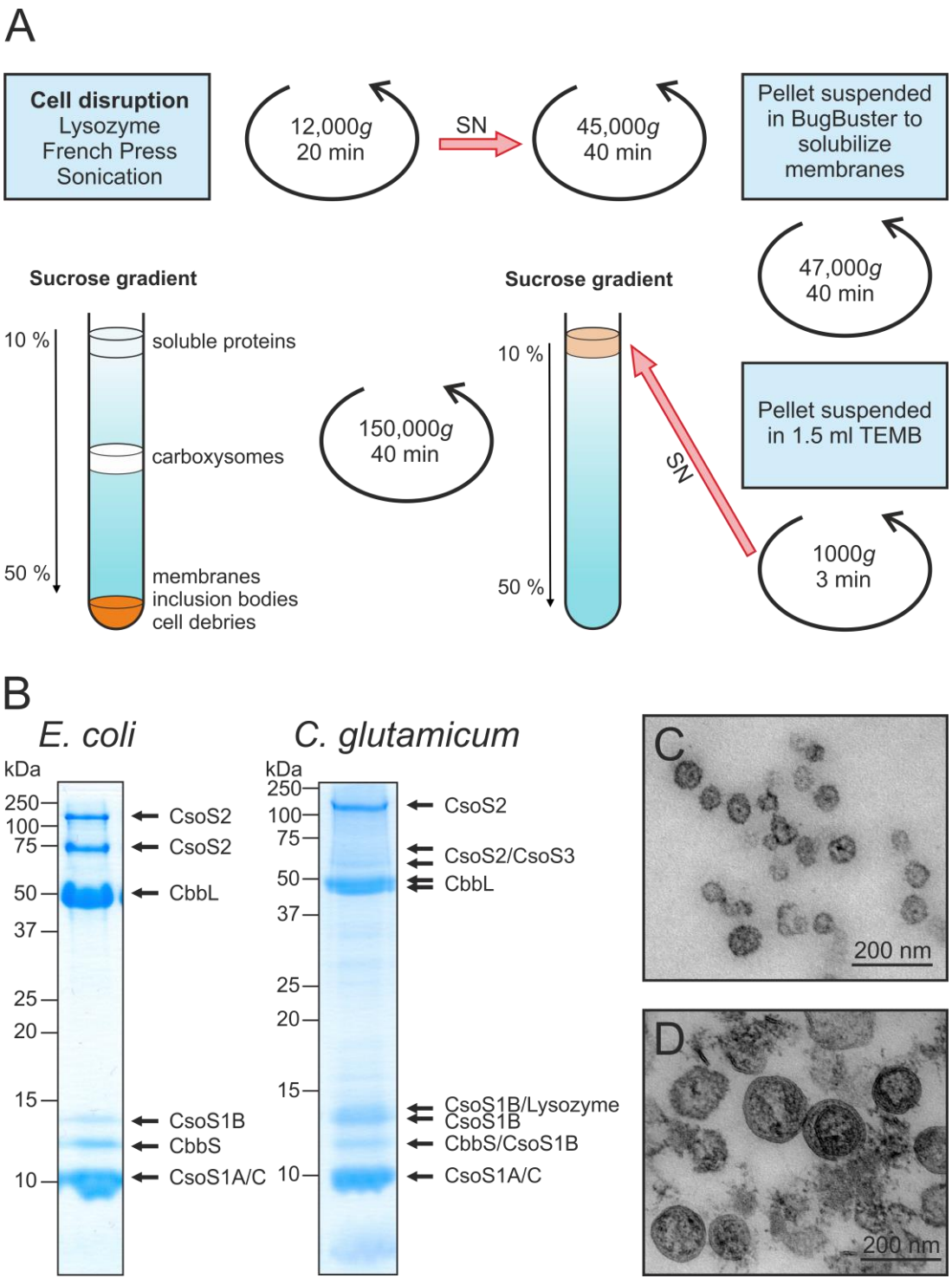

Fig. 2. Carboxysome purification using sucrose gradient centrifugation and TEM pictures of carboxysomes purified from *C. glutamicum* and *E. coli*. (A) Scheme of the carboxysome purification from *C. glutamicum.* For details on the purification procedure, see section 2.4. SN, supernatant. (B) Carboxysomes purified from *E. coli* and *C. glutamicum* carrying pAN6-HNC after the sucrose gradient centrifugation. Presented is an SDS-PAGE of one sample of the middle of the gradient. Positions of marker proteins are indicated. Full pictures of the gradients are presented as Fig. S4. The carboxysomal proteins were identified by MALDI-TOF mass spectrometry. (C) TEM pictures of carboxysomes purified from *C. glutamicum* (C) and *E. coli* (D) at a magnification of ×80,000.

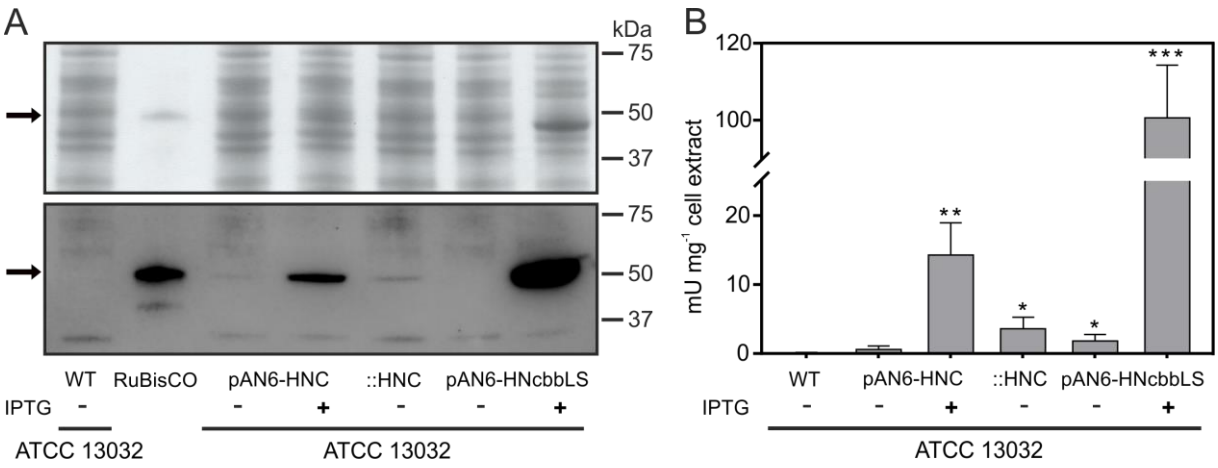

644

645 **Fig. 3.** Production and enzymatic activity of RuBisCO in *C. glutamicum*. The plasmid-based
646 protein production of ATCC 13032 pAN6-HNC and ATCC 13032 pAN6-HNcbbLS under
647 control of P_{tac} was induced with 500 µM IPTG. The expression of the HNC operon in ATCC
648 13032::HNC-whole was under control of the constitutive promoter P_{tuf}. ATCC 13032 without
649 plasmid was used as control (WT). The cells were harvested after 24 h of cultivation in
650 CGXII medium with 2% (w/v) glucose. (A) 20 µg protein of each cell lysate as well as 4 µg
651 RuBisCO were separated by SDS-PAGE (upper panel) and further analyzed by Western blot
652 (lower panel) with antibodies against CbbL. The black arrows indicate the size corresponding
653 to the large subunit of RuBisCO, CbbL (53 kDa). (B) Specific activity of RuBisCO in crude
654 cell extracts. The activities are the mean of three biological replicates. Mean values were
655 compared to the WT (two-tailed Student's t test, n = 3, *$p < 0.05$, **$p < 0.01$, *** $p < 0.001$).
656 One unit is defined as 1 µmol min^{-1} mg^{-1}.

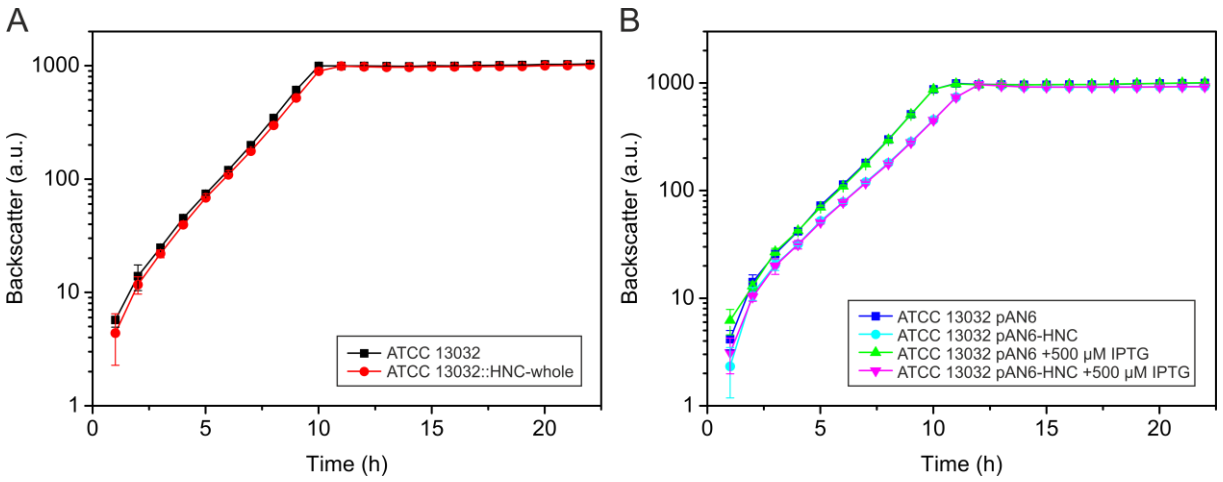

Fig. 4. Growth of *C. glutamicum* expressing carboxysomes either chromosomally (A) or plasmid based (B). The cells were precultivated in BHI medium overnight, washed in PBS buffer and used to inoculate the main cultures consisting of 750 µl CGXII with 2% (w/v) glucose (A) and additionally kanamycin and IPTG as indicated (B).

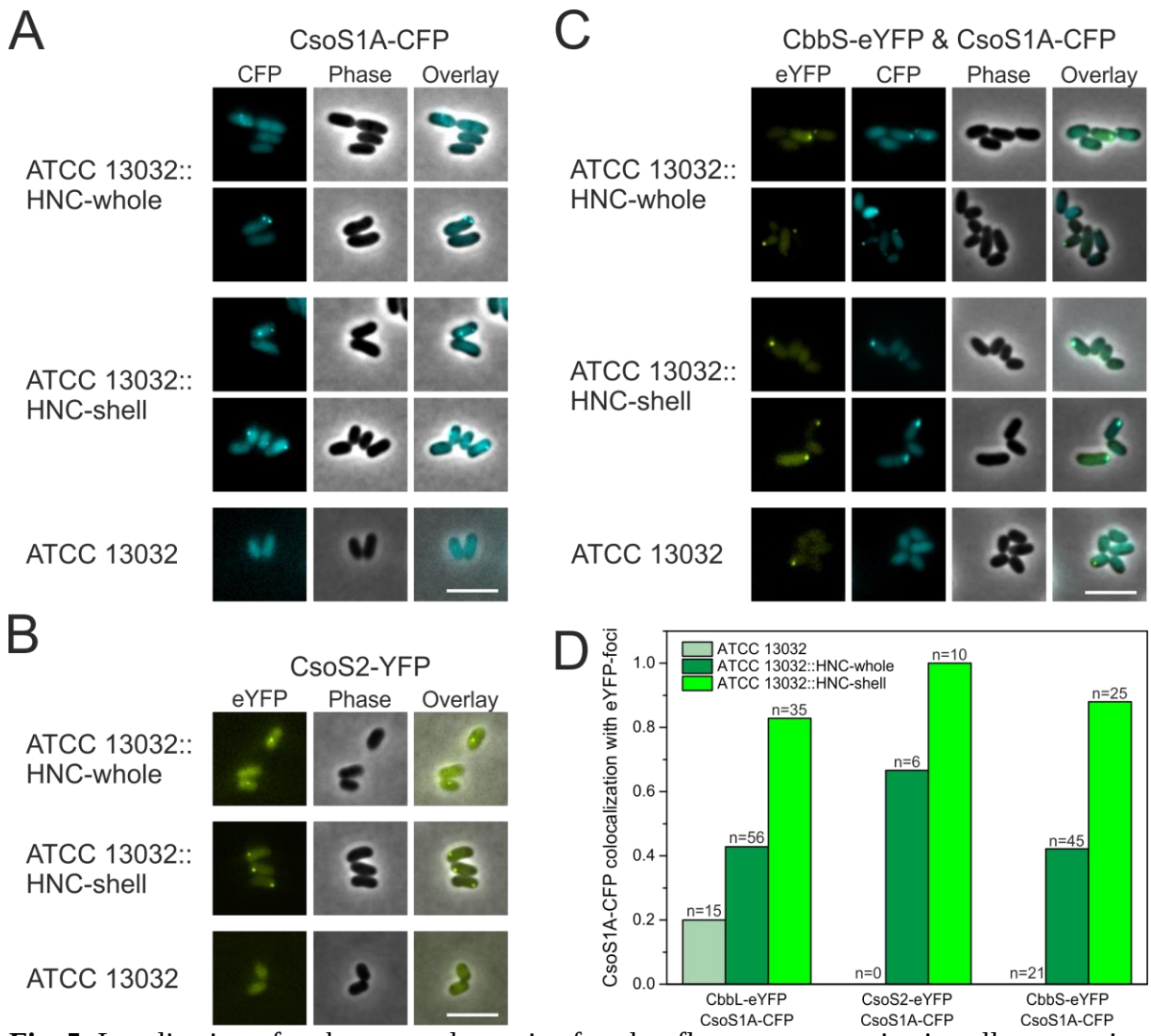

Fig. 5. Localization of carboxysomal proteins fused to fluorescent proteins in cells expressing the native carboxysome operon or only carboxysomal shell genes. After precultivation in BHI media over night the cells were diluted 1:50 into CGXII glucose medium with the required antibiotics and 10 µM IPTG. Fluorescence microscopy was performed after 4-6 h of cultivation. (A) and (B) show the results of cells with a single fusion protein. (C) shows the results of cells expressing two different fusion proteins (CbbS-eYFP and CsoS1A-CFP). (D) summarizes the frequency of co-localized CsoS1A-CFP foci when eYFP foci are present in a cell in different strains. Besides the CbbS-eYFP that is also shown in (C), the localization of CbbL-eYFP and CsoS2-eYFP in combination with CsoS1A-CFP was analyzed. Scale bars 5 µm.

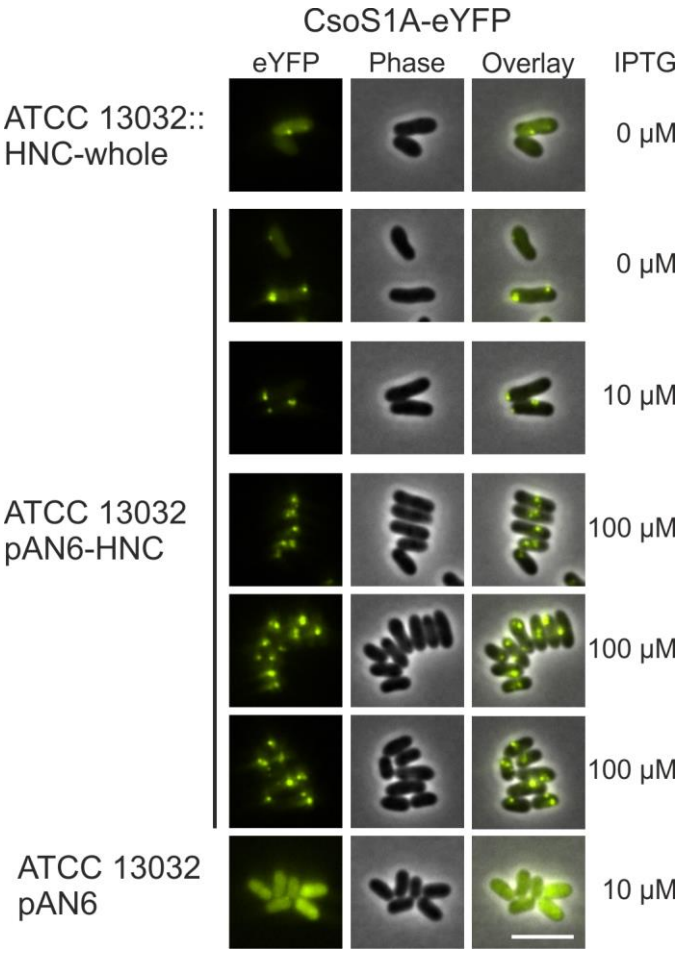

673

674 **Fig.6.** Influence of different induction levels on foci formation in cells expressing the
675 carboxysomal gene cluster. All strains are carrying plasmid pEC-Pacn-CsoS1A-eYFP
676 encoding a fusion protein of CsoS1A and eYFP under control of a constitutive promoter. This
677 plasmid was used to transform ATCC 13032::HNC-whole carrying the chromosomal
678 carboxysome operon under control of a constitutive promoter, ATCC 13032 with the plasmid
679 encoded and inducible carboxysome operon (pAN6-HNC) as well as ATCC 13032 carrying
680 the empty plasmid pAN6 as control. The cells were cultivated as described in the legend of
681 Fig. 5 but chloramphenicol was added to all cultures and kanamycin to all cultures except for
682 ATCC 13032::HNC-whole. Pictures were taken 2 h after start of the main culture. The IPTG
683 amount used for induction of the carboxysomal gene cluster is given on the right. Scale bar 5
684 µm.

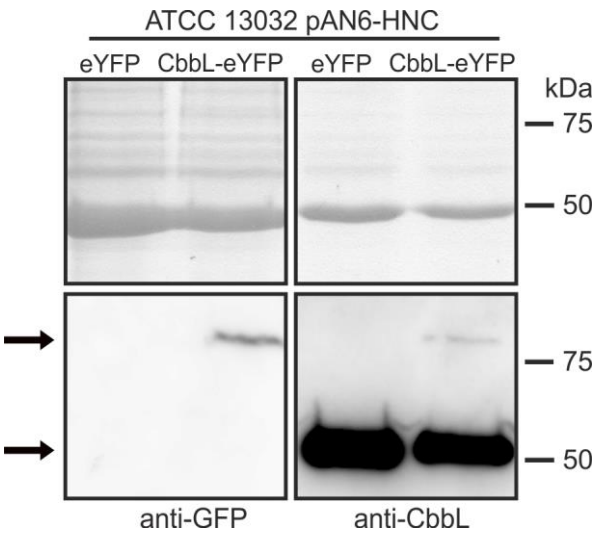

685

686 **Fig. 7.** Co-purification of CbbL-eYFP with carboxysomes. ATCC 13032 was transformed
687 with pAN6-HNC and either or pEC-cbbL-eYFP or pEC-eYFP as control. SDS PAGEs (upper
688 panels) and Western blots (lower panels) of carboxysomes purified from both strains.
689 Presented is for each strain a fraction from the middle of the sucrose gradient. The upper
690 arrow corresponds to the size of CbbL-eYFP with 80 kDa, the lower arrow indicates the size
691 of CbbL with 53 kDa. For the blot probed with Anti-GFP-antibodies, 20 µg proteins were
692 used. For the detection of CbbL, 5 µg proteins were loaded per lane.